Nonlocal thermoelectricity in a Cooper-pair splitter

Robert Hussein,[1] Michele Governale,[2] Sigmund Kohler,[3]
Wolfgang Belzig,[1] Francesco Giazotto,[4] and Alessandro Braggio[4]

[1] *Fachbereich Physik, Universität Konstanz, D-78457 Konstanz, Germany*
[2] *School of Chemical and Physical Sciences and MacDiarmid Institute for Advanced Materials and Nanotechnology, Victoria University of Wellington, P.O. Box 600, Wellington 6140, New Zealand*
[3] *Instituto de Ciencia de Materiales de Madrid, CSIC, Cantoblanco, E-28049 Madrid, Spain*
[4] *NEST, Istituto Nanoscienze-CNR, Piazza S. Silvestro 12, Pisa I-56127, Italy*

(Dated: June 13, 2018)

We investigate the nonlocal thermoelectric transport in a Cooper-pair splitter based on a double-quantum-dot-superconductor three-terminal hybrid structure. We find that the nonlocal coupling between the superconductor and the quantum dots gives rise to nonlocal thermoelectric effects which originate from the nonlocal particle-hole breaking of the system. We show that Cooper-pair splitting induces the generation of a thermo-current in the superconducting lead without any transfer of charge between the two normal metal leads. Conversely, we show a nonlocal heat exchange between the normal leads mediated by non-local Andreev reflection. We discuss the influence of finite Coulomb interaction and study under which conditions nonlocal power generation becomes possible, and when the Cooper-pair splitter can be employed as a cooling device.

PACS numbers: 73.23.Hk, 74.45.+c, 03.67.Bg

I. INTRODUCTION

Hybrid superconductor-semiconductor devices[1–13] are promising candidates for entanglement generation in solid-state systems and, therefore, have potential applications for superconducting spintronics,[14] quantum information and quantum computation.[15,16] The central idea is that the electrons in a s-wave superconductor are in a spin-entangled state which can be made electronically accessible by splitting them via cross-Andreev reflection (CAR) into spatially separated normal leads. The competing process of local Andreev reflection (LAR), where the electrons tunnel into the same lead, does not directly contribute to the spatially nonlocal entanglement. In order to increase the CAR fraction of the current and minimize the effect of LAR, different strategies have been adopted such as employing ferromagnetic leads,[17–21] or including quantum dots with large intradot Coulomb repulsion.[22–28] In double quantum dots with finite Coulomb repulsion, it has been demonstrated that it is possible to induce spatially nonlocal entanglement and manipulate its symmetry by involving only LAR process even without the nonlocal coupling.[29,30]

The study of energy harvesting has also drawn much attention over the last few years.[31–34] Among the suggested implementations using superconductors are S-N junctions,[35] ferromagnet hybrid system,[36–41] and hybrid quantum-dot systems.[42,43] Aspects like thermodynamic efficiencies[44–48] and thermoelectric effects in strongly correlated quantum dots,[49,50] have been addressed. In particular, Machon et al. suggested in Ref. 36 that non-local thermoelectric effects in Cooper pair splitters should exist. Furthermore, Cao et al. showed in Ref. 51 that Cooper-pair splitting can be achieved in the absence of bias voltages by applying a thermal gradient to the normal leads. Inspired by this idea, in this work we present a detailed study of the thermoelectric properties of a Cooper-pair splitter taking fully into account the Coulomb interaction. Further, we discuss the possibility of nonlocal cooling and power generation. Intriguingly, we show that the system still becomes a thermoelectric device due to the influence of the superconducting lead, which by itself is not thermoelectrically active being intrinsically particle-hole symmetric. This is essentially due to the fact that non-local particle-hole symmetry is broken as a consequence of the thermal gradient and the three-terminal device geometry.

This work is organized as follows. In section II, we introduce our model and the formalism employed to calculate the thermoelectric properties. We explore the thermoelectric properties in the linear regime in Sec. III, and compare the results to a simplified effective model. Section IV is devoted to the study of nonlocal power generation and cooling. Finally, we draw our conclusions in section V.

II. MODEL AND MASTER-EQUATION

In this section we introduce the model of the Cooper-pair splitter, sketched in Fig. 1, and the formalism employed to calculate its thermoelectric properties. The Cooper-pair splitter is composed of two quantum dots coupled to a s-wave superconductor and two normal-metal leads, see Ref. 29. For a large superconducting gap, $|\Delta| \to \infty$, the subgap physics is described by the effective Hamiltonian[29,52–58]

$$H_S = H_{\rm DQD} - \sum_{\alpha=L,R} \frac{\Gamma_{S\alpha}}{2}\big(d^\dagger_{\alpha\uparrow} d^\dagger_{\alpha\downarrow} + \text{H.c.}\big) - \frac{\Gamma_S}{2}\big(d^\dagger_{R\uparrow} d^\dagger_{L\downarrow} - d^\dagger_{R\downarrow} d^\dagger_{L\uparrow} + \text{H.c.}\big), \tag{1}$$

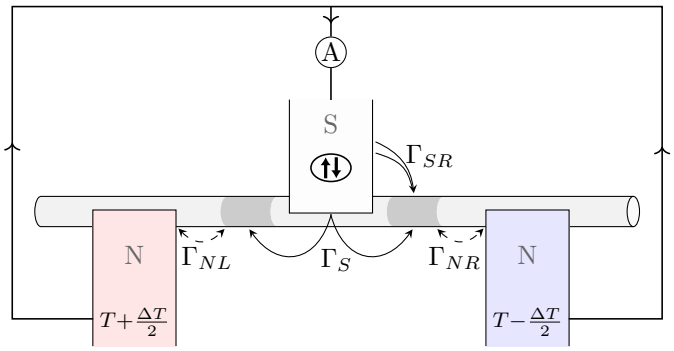

FIG. 1. Cooper-pair splitter circuit consisting of a double quantum dot coupled to two normal leads (N) and a superconducting one (S). A temperature gradient δT between the normal leads induces a nonlocal current into the superconductor which may generate power for finite chemical potentials.

where $H_{\rm DQD}$ describes the double-quantum dot (DQD) system, the second term characterizes the local Cooper-pair tunneling between the superconductor and dot $\alpha = L, R$ with tunneling rates $\Gamma_{S\alpha}$. Here, $d^\dagger_{\alpha\sigma}$ denotes the fermionic creation operator for an electron on dot α with spin $\sigma =\uparrow,\downarrow$. The last term describes the nonlocal tunneling of a Cooper-pair splitting into both dots with the rate $\Gamma_S \sim \sqrt{\Gamma_{SL}\Gamma_{SR}}e^{-l/\xi}$. The non-local coupling Γ_S becomes large when the distance l between both quantum dots is small compared to the coherence length ξ of the superconductor. The DQD is modeled by

$$H_{\rm DQD} = \sum_{\alpha,\sigma}\epsilon_\alpha n_{\alpha\sigma} + \sum_\alpha U_\alpha n_{\alpha\uparrow}n_{\alpha\downarrow} + U\sum_{\sigma,\sigma'} n_{L\sigma}n_{R\sigma'} \quad (2)$$

with ϵ_α the orbital energies and U_α (U) the intradot (interdot) Coulomb interaction; $n_{\alpha\sigma} = d^\dagger_{\alpha\sigma}d_{\alpha\sigma}$ is the occupation operator. We note that in the limit $|\Delta| \to \infty$, the system Hamiltonian is exact in the superconducting coupling Γ_S.[53] This model assumes large single-level spacings in the quantum dots. Hence, a maximum of two electrons with opposite spin can occupy each dot, and in total at most four electrons can reside in the DQD. In the following, we mainly focus on the nonlocal resonance which is not substantially affected by the Coulomb interaction when $U \ll U_\alpha$. In this regime the nonlocal resonance occurs for gate voltages $\epsilon_\alpha \approx -U/2$, as discussed in Ref. 29.

A. Master equation and transport coefficients

For the computation of particle and the heat currents, we restrict ourselves to the sequential tunneling regime, $\Gamma_{NL}, \Gamma_{NR} \ll k_B T_\alpha$, with T_α being the temperature of the normal lead α. In this regime, the populations P_a of the eigenstates of the system, $|a\rangle$, obey a Pauli-type master equation of the form[29] $\dot{P}_a = \sum_{a'}(w_{a\leftarrow a'}P_{a'} - w_{a'\leftarrow a}P_a)$ with the stationary solution denoted as $P^{\rm stat}_a$. The transitions rates for tunneling of an electron from the normal lead α to the respective dot ($s = +1$) and the opposite processes ($s = -1$) are simply given by Fermi's golden rule

$$w^{(\alpha,s)}_{a\leftarrow a'} = \sum_\sigma \Gamma_{N\alpha} f^{(-s)}_\alpha(-s\omega_{aa'})|\langle a|d^{(-s)}_{\alpha\sigma}|a'\rangle|^2, \quad (3)$$

with the notation $d^{(-s)}_{\alpha\sigma}$ for the electron creation and annihilation operators and $f^{(s)}_\alpha(\epsilon) = \{1 + \exp[s(\epsilon - \mu_\alpha)/k_B T_\alpha]\}^{-1}$ for the Fermi function at chemical potential μ_α. Hence, the total rates entering the master equation are given by

$$w_{a\leftarrow a'} = \sum_{\alpha,s=\pm} w^{(\alpha,s)}_{a\leftarrow a'}. \quad (4)$$

The electron and heat currents through the contacts correspond to the rates of changes of the particle number and the energy in the corresponding lead, $I_\alpha \equiv e_0\langle\dot{N}_\alpha\rangle$ and $\dot{Q}_\alpha \equiv \dot{E}_\alpha - \frac{\mu_\alpha}{e_0}I_\alpha$, respectively. The last term in the expression of the heat current reflects the fact that in order to obtain the heat current, one needs to subtract the net energy associated with the flux of particles at the fixed electrochemical potential μ_α. In the sequential-tunnelling regime with the normal metal leads it is easy to write the currents in terms of the stationary populations of the DQD $P^{\rm stat}_{a'}$ and the rates $w^{(\alpha,s)}_{a\leftarrow a'}$:

$$I_\alpha = \frac{e_0}{\hbar}\sum_{a,a',s=\pm} s w^{(\alpha,s)}_{a\leftarrow a'} P^{\rm stat}_{a'} \quad (5)$$

$$\dot{Q}_\alpha = -\frac{1}{\hbar}\sum_{a,a',s=\pm} s(E_a - E_{a'}) w^{(\alpha,s)}_{a\leftarrow a'} P^{\rm stat}_{a'} - \frac{\mu_\alpha}{e_0}I_\alpha. \quad (6)$$

For the superconducting leads, the electric current is determined by current conservation, that is $I_S = -I_L - I_R$. In the large gap limit, due to perfect Andreev heat mirroring, the heat transferred to the superconductor vanishes, i.e. $\dot{Q}_S = 0$. This means that the heat current in the system flows only between the normal leads.

In thermoelectrical systems, it is instructive to discuss the linear regime at small voltage $\delta V = (\mu_R - \mu_L)/e_0$ and small thermal bias $\delta T = T_L - T_R$, where the transport coefficients are defined by the relations

$$\delta I_S = L^S_{11}\delta V + L^S_{12}\delta T, \quad (7)$$

$$\delta\dot{Q}_R = L^R_{21}\delta V + L^R_{22}\delta T. \quad (8)$$

Beyond the linear regime, Onsager coefficients of higher order[59,60] $L^S_{kk'}$, $L^R_{kk'}$ can be calculated by recursive methods.[61] The master-equation formalism presented so far can be easily generalized to compute higher-order current cumulants by using standard full-counting-statistics techniques and introducing appropriate counting variables both for the charge and energy currents.[61–65] Hereafter, we only consider the average currents since these are the quantities that are easily accessible experimentally.

III. THERMOELECTRICITY AT ZERO BIAS VOLTAGE

Hereafter, we will discuss the nonlocal thermoelectrical behavior of the Cooper-pair splitter for intradot Coulomb energies U_R and U_L much larger than any other energy scale, such that double occupancy of each indivual dot is energetically forbidden. This simplifies the system making the physics more transparent.[66] In order to investigate thermoelectrical effects, we assume that the normal leads are at different temperatures, $T_L > T_R$. We focus on the following non-local thermoelectrical effect: a thermal gradient between the normal leads induces a charge current between the superconductor and the normal leads, see Fig. 1, even if the chemical potentials of the three leads are kept equal, $\mu_S = \mu_R = \mu_L = 0$. In the limit $U_R, U_L \gg \epsilon_R, \epsilon_L \approx 0$, the current through the superconducting lead I_S is purely induced by nonlocal Cooper-pair splitting, $I_S < 0$, and recombination, $I_S > 0$, respectively. In the former(latter) process Cooper pairs, consisting of electron singlets, split into (recombine from) different dots. Since only non-local Andreev reflection is present, the average currents through both normal leads are identical, $I_R = I_L = -I_S/2$, irrespectively of the lead temperatures and tunnel couplings.

Furthermore, since we consider the situation of a large superconducting gap, $|\Delta| \to \infty$, no quasiparticle excitation can take place and heat transfer within the superconducting lead is forbidden. Thus, heat transfer can only occur between the two normal leads mediated by the superconducting lead, which operates as a perfect nonlocal Andreev mirror.

In Fig. 2(a), we show a density plot of the superconducting current I_S as a function of the level energies ϵ_R and ϵ_L for temperatures much smaller than the nonlocal coupling, $k_B T_\alpha \ll \Gamma_S$. We recognize immediately that the current is finite for $\epsilon_R \neq \epsilon_L$. The current is non-vanishing close to the dashed lines corresponding to the resonance conditions $2\Delta E_\pm = \epsilon_L - \epsilon_R \pm \sqrt{(\epsilon_L + \epsilon_R)^2 + 2\Gamma_S^2} = 0$.

The addition energies, $\Delta, E_\pm$ correspond to processes of electron exchange at the normal leads for the model Hamiltonian

$$H_{\text{eff}} = \sum_{\alpha\sigma} \epsilon_\alpha \Big(|\alpha\sigma\rangle\langle\alpha\sigma| + \frac{|S\rangle\langle S|}{2} \Big) - \frac{\Gamma_S}{\sqrt{2}} \big(|0\rangle\langle S| + |S\rangle\langle 0| \big) \quad (9)$$

involving the empty state $|0\rangle$, the singly occupied states $|\alpha\sigma\rangle = d^\dagger_{\alpha\sigma}|0\rangle$ of dot $\alpha = L, R$ with spin $\sigma = \uparrow, \downarrow$, and the singlet state $|S\rangle = \frac{1}{\sqrt{2}}\big(d^\dagger_{R\uparrow} d^\dagger_{L\downarrow} - d^\dagger_{R\downarrow} d^\dagger_{L\uparrow}\big)|0\rangle$. In the Hamiltonian we have omitted the triplet states as they cannot be directly coupled to the superconductor, where only singlet Cooper pairs are present. The triplet states play an important role in the high-bias regime, yielding a suppression of the current called triplet blockade.[54]

In Fig. 2(b), we consider the heat flow from the hot to the cold normal lead. Essentially, non-vanishing heat flow occurs where the thermo-electrical behavior is present, indicating that the mechanism of thermo-electricity in the system is also responsible for the heat exchange. Intriguingly, here the heat exchange is mediated only by Cooper pairs, since there is no other way for an excitation to be transferred from one normal lead to another without a process involving a Cooper emission or absorption at the superconducting interface. As expected, Cooper pair cannot transfer heat to/from the superconductor, being at zero energy (ground state), but they can coherently mediate heat exchange between the normal leads. We refer to this mechanism as *nonlocal heat-exchange* coherently mediated by the superconducting lead. This interpretation is supported by the fact that the heat exchanged is enhanced just inside the gap between the two resonances, see Fig. 2(b). Indeed, inside the gap for $\epsilon_R, \epsilon_L \approx 0$ the heat current remains finite. This is a consequence of the fact that the contributions of the two nearby resonances have opposite particle/hole character and add up. Conversely, the thermo-electrical current is suppressed in the gap since particles and holes have opposite charges and, consequently, yield opposite contributions to the thermoelectrical current. It is important to stress that this heat transfer mediated by the superconductor does not affect the superconducting state and can be interpreted as a non-local version of the Andreev mirror phenomena for heat current.

In panels (c,d) of Fig. 2, we consider the linear regime in temperature $\delta T \ll T = (T_L + T_R)/2$. In this case, the linear transport coefficients depend only on the average temperature T of the leads. We now discuss how the linear coefficients L_{12} and L_{22} vary with the detuning $\Delta\epsilon \equiv \epsilon_R - \epsilon_L$ along the line $\epsilon_L = -\epsilon_R$ when changing the temperature but keeping fixed the nonlocal coupling Γ_S, which determines the distance between the two resonances.

In Fig. 2(c) the two central (inner) peaks progressively cancel each other as the temperature increases. This is a consequence of the fact that when $\Gamma_S \gtrsim k_B T$, the electron-like contribution of one resonance coexists with the hole-like of the other resonance. This competition reduces the total thermoelectric current. Once $k_B T = \Gamma_S$ the two resonances merge and behave as a single resonance. Panel (d) shows the corresponding linearized heat current coefficient L^R_{22}. For well separated peaks, $\Gamma_S \gg k_B T$, the heat current essentially vanishes at the resonances, where also the current coefficient vanishes. In the situation when the peaks are in proximity, $\Gamma_S \gtrsim k_B T$, they add up constructively at $\Delta\epsilon \approx 0$. When $k_B T = \Gamma_S$ again the thermal behavior resembles the contribution of a single QD resonance.

In the following, we develop a physical picture to explain the behavior of the linear thermoelectric coefficients in the limit of large intradot Coulomb interaction, for equal chemical potentials, $\mu \equiv \mu_L = \mu_R$ and in the presence of a temperature gradient between the two normal leads, $T_L > T_R$. Figure 3(a) depicts the level structure of the double quantum-dot system in the situation where the chemical potentials of the normal leads coin-

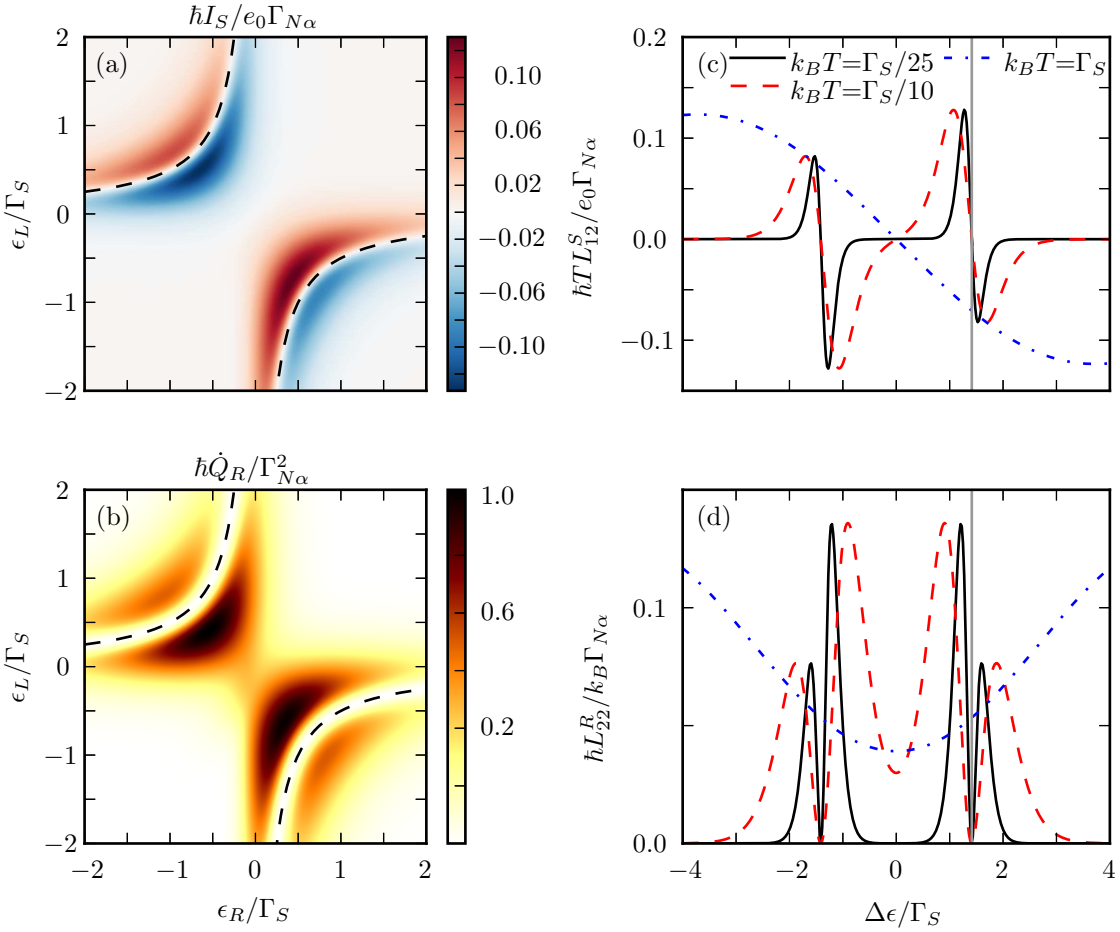

FIG. 2. (a) Superconducting current $I_S = -I_L - I_R$ and (b) heat current $\dot{Q}_R$ through the right normal lead as a function of the level energies ϵ_L and ϵ_R. Parameters are $k_BT_L = 15\Gamma_{N\alpha}$, $k_BT_R = 5\Gamma_{N\alpha}$, $\Gamma_S = 100\Gamma_{N\alpha}$, $U = t = \mu_\alpha = \Gamma_{S\alpha} = 0$, and $U_\alpha \gg \Gamma_S$. The dashed lines indicate where the Andreev bound state addition energies $\left[(\epsilon_L - \epsilon_R) \pm \sqrt{2\Gamma_S^2 + (\epsilon_L + \epsilon_R)^2}\right]/2$ are resonant with the Fermi levels at $\mu = 0$. (c,d) Linear current coefficient L^S_{12} and heat current coefficient L^R_{22} in the limit $\delta T \equiv T_L - T_R \to 0$ as a function of the detuning $\Delta\epsilon \equiv \epsilon_R - \epsilon_L$ for different average temperatures T. Here, the energy levels are symmetrically detuned, i.e. $\epsilon_R = -\epsilon_L$. The vertical line indicates one of the Andreev bound state addition energies.

cide with the one of the superconductor. For $\epsilon_L, \epsilon_R \approx 0$ the singlet state mixes with the empty state forming a non-local Andreev bound states shared between the two dots due to nonlocal Cooper-pair tunneling with the central superconducting lead.[67] The electron tunneling with the normal leads determines transition between the DQD state. The dotted lines indicate the Andreev bound state addition energies $\Delta E_\pm$, while the solid lines with a Lorentzian-like resonance indicate the broadened energy levels of the quantum dots with the natural linewidth $\gamma \approx \Gamma_{NL} + \Gamma_{NR}$.

In the case that more electrons are above the Fermi level of the left normal lead than holes below the Fermi level of the right normal lead, electrons tunnel via the Andreev bound-state channel into the superconductor and form Cooper pairs (red arrows). At the same time Cooper pairs can split in an opposite process and tunnel into the normal leads (blue arrows). The difference of both processes yields a net thermoelectrical current when the normal leads have different temperatures. This effect is a direct consequence of the nonlocal particle-hole asymmetry induced by the structure.

In Fig. 4 we show the dependence of the linear coefficients on the non-local coupling Γ_S keeping fixed the temperature T. Theis behavior can be captured by mapping the Cooper-pair splitter in the CAR regime to a simplified model of a single quantum dot with two resonances located at the addition energies of the Andreev bound states. The thermoelectrical coefficients of this simplified model can be then expressed in the Landauer-Büttiker formalism as[68–72]

$$L^{\text{eff}}_{k+1,2} \equiv \frac{(2e_0)^{1-k}}{h} \int_{-\infty}^{\infty} dE \, \frac{E^{k+1}\tau(E)}{4k_BT^2 \cosh^2\left(E/2k_BT\right)}. \tag{10}$$

The additional factor 2 for the electron current ($k = 0$) takes into account that in an Andreev process the current is doubled ($I_S = -2I_R$). The transmission function

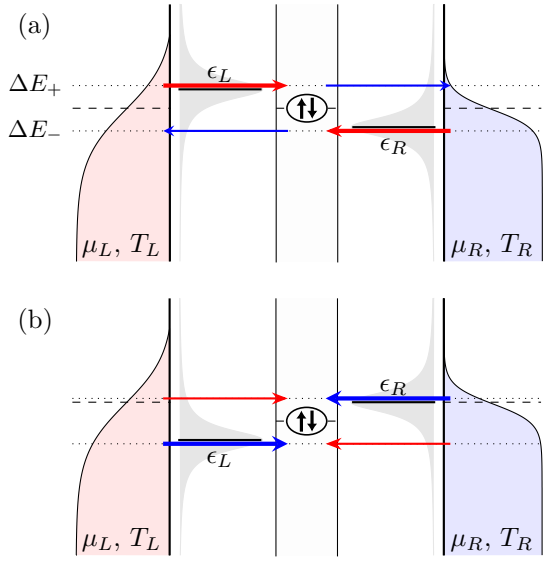

FIG. 3. (a) Cooper-pair splitter configuration for zero chemical potentials, $\mu_L = \mu_R = 0$, leading to a heating of the right normal lead and a net current into the superconductor. (b) Configuration for finite chemical potentials, $\mu_L = \mu_R > 0$, applied over the junction, cause a net current into the superconductor against the intrinsic thermo-current leading to a cooling of the left normal lead.

is modeled as two Lorentzians located at the Andreev bound state energies

$$\tau(E) \propto \sum_{s=\pm} \frac{\gamma}{(E - \Delta E_s)^2 + (\gamma/2)^2}. \tag{11}$$

Finally one arrives at $L^{\text{eff}}_{k+1,2} = \alpha \frac{(2e_0)^{1-k}}{\hbar} \sum_{s=\pm} A_k(\Delta E_s)$ with α an overall scaling factor and the function

$$A_k(\Omega) = \sum_{s=\pm} \frac{\omega_s^{k+1}(\Omega)}{k_B(2\pi T)^2} \Psi'\Big(\frac{1}{2} - \frac{si\omega_s(\Omega)}{2\pi k_B T}\Big) + \frac{\gamma\delta_{k,1}}{2\pi T}, \tag{12}$$

which collects the contributions from the poles of the Fermi function and the poles $\omega_s(\Omega) = \Omega + si\gamma/2$ of the Lorentzians. Here, Ψ denotes the digamma function.

The reader should be aware that in the quantum dot model the thermo-electrical current and the thermal current flow always between the two normal leads instead in our system, due to the presence of the superconducting lead with non-local coupling, the charge and thermal current flow in different terminals.[73]

In figure 4, we compare the linear thermoelectric coefficient (panel a) and thermal conductance (panel b) of this simplified model (dashed lines) with the results of the full calculation (solid lines) for different nonlocal couplings Γ_S as a function of the detuning. Here, the factor α of the effective quantum-dot model has been chosen such that the linear current coefficient at $\Gamma_S = k_B T$ fits the one of the full model. The model qualitatively captures the curve progression of the full computation. When the nonlocal coupling is much larger than temperature

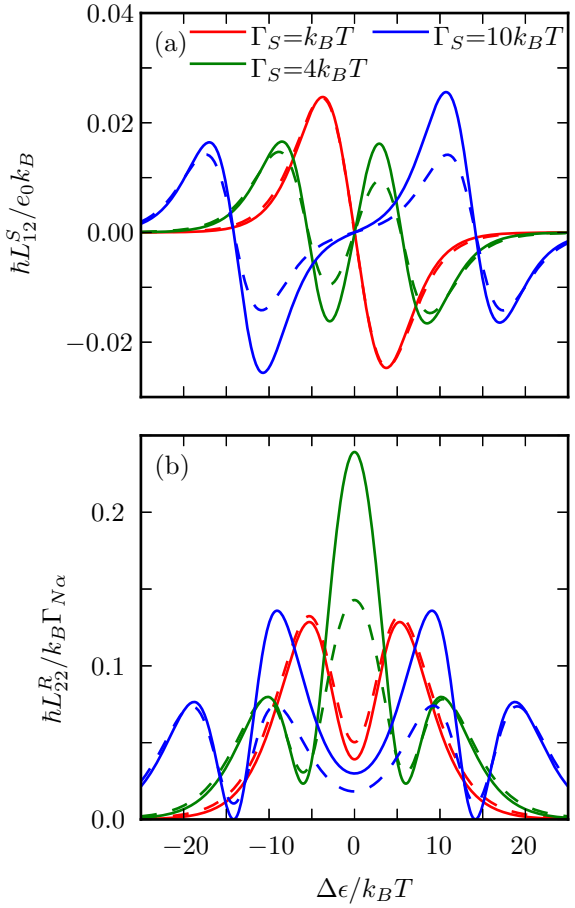

FIG. 4. (a) Linear current and (b) heat current coefficients L^S_{12} and L^R_{22} as a function of the detuning $\Delta\epsilon$ with the average temperature $T = 5\Gamma_{N\alpha}/k_B$ and all other parameters as in Fig. 2(a). The dashed lines correspond to the effective model, see Eqs. (10), scaled by a factor of $\alpha = 0.37$, such, that the effective linear current coefficient agrees with the one of the full model for $\Gamma_S = k_B T$.

(blue lines) the behaviour exhibits two well separated resonance. At $\Gamma_S = 4k_BT$ (green lines), the heat transport around zero detuning is enhanced and this can be understood by the additive superposition of the contributions of both Lorentzians. For lower values of the non-local coupling (red lines) the two resonances effectively merge and the behavior resembles that of a single resonance with a minimum in the thermal conductance at zero detuning. A measurement of the maximum $\Gamma_S = 4k_BT$ of the thermal current at the resonance $\Delta\epsilon = 0$ as a function of temperature is an indirect way to measure the strength of the non-local coupling.

A few comments on the origin of the deviation between the full result (solid lines) and the simplified model (dashed lines) are in order. In the simplified model, the peaks around the resonances of the thermo-electrical coefficient, see Fig. 4(a), are symmetric; this is not the case for the full results. The reason for the asymmetry is that the two resonances correspond to different Andreev lev-

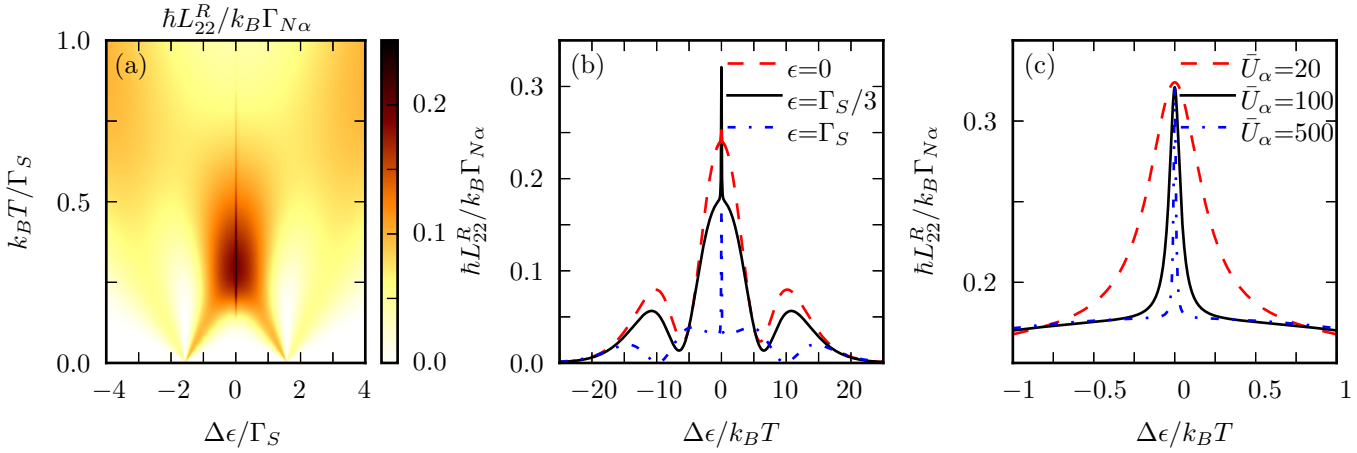

FIG. 5. (a) Linear heat current coefficient L^R_{22} (which for $\delta V = 0$ is proportional to the heat current $\dot{Q}_R$) as a function of the detuning $\Delta\epsilon$ and the average temperature T for finite intradot Coulomb energy $U_\alpha = 100\Gamma_{S\alpha}$, $\Gamma_S = \Gamma_{S\alpha}/3 = 4k_BT$ and $k_BT = 10\Gamma_{N\alpha}$. Here, the level energies $\epsilon_L = \epsilon - \Delta\epsilon/2$ and $\epsilon_R = \epsilon + \Delta\epsilon/2$ are centered around the average value $\epsilon = \Gamma_S/3$. (b) Dependence on the average level energies ϵ and (c) the interdot couplings $\bar{U}_\alpha \equiv U_\alpha/\Gamma_{S\alpha}$.

els and this implies different energy-dependent weighting factors in front of the Lorentzians.[74] Similarly, for the thermal conductance, panel (b), the simplified model underestimates the height of the central peak. This can be again attributed to the fact that the central peak comes from the combined action of the two Andreev resonances and not from independent resonances as naively postulated in the simplified model. The differences between the two models are a specific signature of the nature of the Andreev bound states in the DQD system with respect to standard QD resonances. This justifies our approach for the investigation of thermoelectrical quantities.

We conclude this section with a final remark on the possibility to obtain a cooling cycle. When a thermoelectrical device is operated near the reversibility condition, the thermo-electrical cycle can be inverted in order to get a cooling cycle. Inspecting the level structure sketched in Fig. 3(b) one expects nonlocal cooling at finite chemical potential. The reason is that in this case it is possible to have more electrons in the right normal lead above the CAR then holes in the left normal lead below (blue arrows), resulting in the cooling of the right normal lead. The condition $f_R(\Delta E_\pm) = 1 - f_L(-\Delta E_\mp)$ determines where for a certain temperature difference δT and for fixed bias μ, the thermoelectrical current is zero. This condition, defined for the simplified model, roughly determines the Seebeck potential of the system which can be estimated to be approximately

$$\mu_\mp \approx \epsilon + \left(\Delta\epsilon \mp \sqrt{2}\Gamma_S\right)\frac{\delta T}{4T}\,, \tag{13}$$

where we have used the parametrization $\epsilon_{L,R} = \epsilon \mp \Delta\epsilon/2$. At these values of the chemical potential we find that nonlocal heating turns into nonlocal cooling and our thermoelectrical engine becomes a cooler. We return to this point in Sec. IV, where we address quantitatively for the full model the possibility of power generation and cooling, and see that nonlocal cooling, indeed, sets in at $\mu \approx \mu_\mp$.

However before doing so, we discuss in the following the effect of finite Coulomb interaction on the transport properties at the nonlocal resonance.

A. Effect of finite Coulomb interaction

Thus far, we have restricted our analysis to the case of infinite local Coulomb interaction in the QDs, so that the double occupation of the individual dots is forbidden. Relaxing this condition and considering finite values for U_α opens up the possibility of a local exchange of Cooper pairs between the superconductor and the system (both electrons in the Copper pair tunnel to/from the same dot).[75] This includes the possibility to consider different virtual transitions involving a nonlocal resonance. In this way, electrons can transfer energy between the normal leads via elastic cotunneling. Thus, the finite intradot Coulomb interaction can increase the heat current $\dot{Q}_R$, while the current I_S through the superconductor remains unaffected. In particular, an electron with spin σ above the chemical potential of the left normal lead may tunnel with the rate Γ_{NL} into the left dot and occupy the state $|L\sigma\rangle$. Then a Cooper-pair may split nonlocally with the coupling Γ_S into the triply occupied state $|tR\sigma\rangle = d^\dagger_{R\sigma}d^\dagger_{L\uparrow}d^\dagger_{L\downarrow}|0\rangle$ followed by a local Cooper-pair recombination with the rate Γ_{SL}. Finally, the electron leaves the dot with the rate Γ_{NR} via the right normal lead, heating up the right lead. The process can also proceed differently with the local coupling operating before the nonlocal one. In this process the electron is effectively transferred to the state $|R\sigma\rangle$ of the right dot with no net current in the superconductor. This shows again that, due to nonlocality, the resonant behaviour of the heat does not necessarily affect the charge current. The

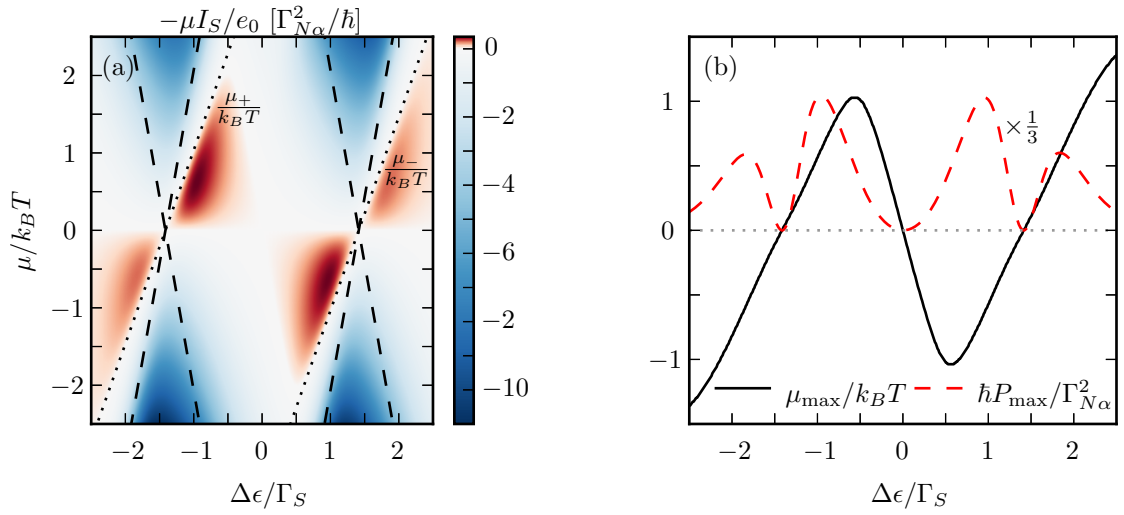

FIG. 6. (a) Thermopower $P = -\mu I_S/e_0$ as a function of the detuning $\Delta\epsilon \equiv \epsilon_R - \epsilon_L$ and the chemical potential $\mu \equiv \mu_L = \mu_R$, choosing the average level energy to be zero, i.e. $\epsilon_R + \epsilon_L = 0$. The parameters are chosen as in Fig. 2(a). The dashed lines indicate where the addition energies $\Delta E_\pm$ are in resonance with the chemical potential μ, while the dotted lines correspond to the estimated Seebeck potential $\mu_\pm$ given in Eq. 13. (b) Maximal power $P_{\max} = \max_\mu P(\Delta\epsilon, \mu)$ (dashed line) and chemical potential $\mu_{\max}$ corresponding to the maximal power (solid line) for fixed detuning.

aforementioned mechanism can be identified in the thermal transport at finite interaction such as in Fig. 5(a), where the thermal transport coefficient L_{22}^R is shown as a function of the detuning $\Delta\epsilon$ and the average temperature T. The thermal conductance L_{22}^R describes how the heat current flows between the two normal terminals for $\mu = 0$. A remarkable feature is the narrow resonance at $\Delta\epsilon = 0$. This resonance is absent for infinite local Coulomb interactions and its linewidth increases with the scaling Γ_α/U_α, indicating its origin in the elastic cotunneling mechanism.

In Fig. 5(c) we show that for increasing intradot Coulomb interaction, the cotunneling peak becomes narrower, while its height remains unaffected. For this calculations the average quantum dot level has been chosen to be $\epsilon \equiv (\epsilon_L + \epsilon_R)/2 = \Gamma_S/3$ as since for $\epsilon = 0$ the resonance is less pronounced [panel (b)].

IV. NONLOCAL THERMOELECTRIC POWER

So far, we have studied the transport coefficients for equal chemical potentials $\mu_R = \mu_L = \mu_S = 0$. In this case there is no power generation. For any circuital element electrical work is performed, if the charge carriers gain potential energy in the by flowing against an increasing chemical potential. Therefore, while keeping the chemical potential of the superconductor at zero, for reference, we now consider normal leads at non-zero values of μ. The corresponding generated work or thermopower $P \equiv -\mu I_S/e_0$ reflects the potential energy that an electron gains.[76] Upon increasing μ from a finite value that still allows such counter-flow to even larger values, at some value the flow will come to a standstill. Increasing μ further, will change the sign of the current. Then the thermoelectric element becomes dissipative and the electrons flow in the direction of the potential drop. In the inverted regime cooling effect can also be found before, at even higher voltages, a fully dissipative regime dominates.

Figure 6(a) shows the nonlocal thermopower as a function of the chemical potential and the detuning. Obviously for sufficiently large absolute values of μ, the current becomes dissipative (negative power) as expected. Nevertheless, there exist regions, namely the triangular ones in red, in which the Cooper pair splitter effectively generates positive thermopower and acts as a thermogenerator. In Fig. 6(b), we show the maximum generated power $P_{\max}$ (red dashed line) and the corresponding Seebeck potential $\mu_{\max}$ (solid line) for which this maximum is obtained. The maximum generated power is relatively small, $P_{\max} \approx \Gamma_{N\alpha}^2/3\hbar$, and decaying for large detuning.

Finally we discuss the thermoelectric efficiencies for power generation and cooling. For the nonlocal power generation, the efficiency $r_{\text{eng}} = (P/|\dot{Q}_L|)/\eta_C$ is given by the power $P > 0$ generated in the system per extracted heat flow $-\dot{Q}_L > 0$ from the warmer normal lead.[48] It is normalized to the Carnot efficiency of a heat engine $\eta_C = 1 - T_R/T_L$, which is bounded between 0 and 1. Similarly, the cooling power $r_{\text{fri}} = \left(\dot{Q}_R/P\right)/\eta_{\text{fri}}$ is defined as the heat flow $\dot{Q}_R < 0$ extracted from the cold reservoir per absorbed power. We compare it with the ideal efficiency of a refrigerator $\eta_{\text{fri}} = T_R/(T_L - T_R)$, which can be larger than one. The combined efficiency

$$r_{\text{therm}} = \begin{cases} r_{\text{eng}}, & P > 0 \\ -r_{\text{fri}}, & \dot{Q}_R < 0 \end{cases} \tag{14}$$

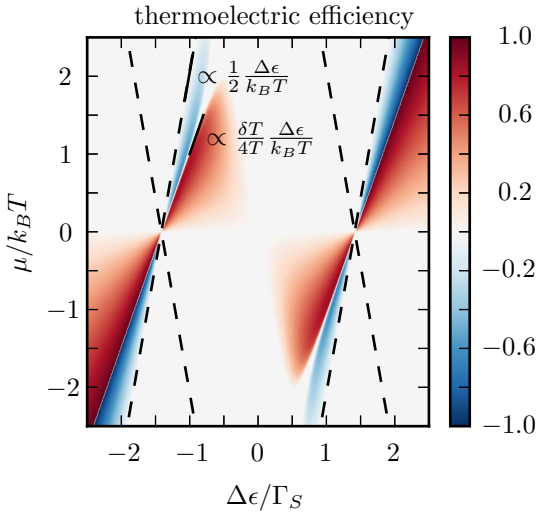

FIG. 7. Power generation efficiency $P/(-\dot{Q}_L)$ (red) for $P > 0$, and cooling efficiency $\dot{Q}_R/P$ (blue) for $\dot{Q}_R < 0$ normalized by the corresponding Carnot efficiencies, see Eq. (14). In order to depict both efficiencies in the same plot, the latter is multiplied by a factor of -1. All parameters are as in Fig. 6.

is depicted in Fig. 7 as a function of the detuning and the chemical potential, where positive values (red) correspond to power generation and negative values (blue) to cooling of the right normal lead. Close to the lines where the thermoelectric current vanishes, $\mu \propto (\delta T/4T)\Delta\epsilon$ see Eq.(13), the system has a very high efficiency and represents an almost reversible thermoelectric generator (red shaded area). However, the power generated under this condition is rather small. Therefore, as usual, there is a trade-off between high efficiency and high output.

The fact that the thermal machine operates nearly at the Carnot efficiency for some finite $\mu \neq 0$, suggests that the system can become a cooling device. This happens, indeed, in the blue shaded region bounded by the nonlocal Andreev resonance at $\mu \propto \Delta\epsilon/2$, where the colder lead is further cooled due to nonlocal Cooper-pair tunneling.

V. CONCLUSIONS

Nonlocal thermoelectric effects in a double-dot Cooper-pair splitter have been investigated. Thermoelectricity properties are determined by the non-local breaking of the particle-hole symmetry which is realized in the hybrid three-terminal structure in the presence of a temperature gradient. Intriguingly, we demonstrated that the superconductor can mediate coherent heat transfer between the normal leads. The rich phenomenology can be easily interpreted in terms of a simple model consisting of two resonances located at the nonlocal Andreev bound state addition energies. However, this model has some limitations and the full model is required to get accurate results for the thermal transport. In particular the Andreev nature of the resonances is reflected in different energy dependence of those resonances. In particular, in comparison to the model, one predict an enhancement of heat transferred between the normal lead at resonance for $\Gamma_S = 4k_BT$. Finally at nonlocal resonance for finite Coulomb interaction an extra resonance is located in the heat transport as a consequence of virtual transition to triple occupied states. When applying a load between the normal leads and the superconducting one, the Cooper-pair splitter can perform work and convert heat current into electric current with nearly Carnot efficiency. The detuning can be used as control knob to turn the nonlocal power generator to a heat pump and cool the colder normal lead via nonlocal Cooper-pair tunneling.

ACKNOWLEDGMENTS

When writing this paper, we became aware of a related work by Rafael Sánchez et al. 77.

R.H. acknowledges financial support from the Carl-Zeiss-Stiftung. This work was supported by the Spanish Ministry of Economy and Competitiveness via Grants MAT2017-86717-P and MAT2016-82015-REDT. W.B. acknowledges financial support from the DFG through SPP 2137 "Spin Caloric Transport". A.B. and F.G. acknowledge the European Research Council under the European Union's Seventh Framework Program (FP7/2007-2013)/ERC Grant agreement No. 615187-COMANCHE and the Tuscany Region under the FARFAS 2014 project SCIADRO for partial financial support. A.B. acknowledges the CNR-CONICET cooperation programme "Energy conversion in quantum nanoscale hybrid devices" and the Royal Society through the International Exchanges between the UK and Italy (grant IES R3 170054). M.G. acknowledges the hospitality of Scuola Normale Superiore, Pisa.

[1] G. B. Lesovik, T. Martin, and G. Blatter, Eur. Phys. J. B **24**, 287 (2001).
[2] S. Russo, M. Kroug, T. M. Klapwijk, and A. F. Morpurgo, Phys. Rev. Lett. **95**, 027002 (2005).
[3] A. Martín-Rodero and A. L. Yeyati, Adv. Phys. **60**, 899 (2011).
[4] S. Roddaro, A. Pescaglini, D. Ercolani, L. Sorba, F. Giazotto, and F. Beltram, Nano Res. **4**, 259 (2011).
[5] F. Giazotto, P. Spathis, S. Roddaro, S. Biswas, F. Taddei, M. Governale, and L. Sorba, Nature. Phys. **7**, 857 (2011).
[6] J. Schindele, A. Baumgartner, and C. Schönenberger, Phys. Rev. Lett. **109**, 157002 (2012).

[7] L. Romeo, S. Roddaro, A. Pitanti, D. Ercolani, L. Sorba, and F. Beltram, Nano Lett. **12**, 4490 (2012).
[8] A. Das, Y. Ronen, M. Heiblum, D. Mahalu, A. V. Kretinin, and H. Shtrikman, Nature Commun. **3**, 1165 (2012).
[9] B. Braunecker, P. Burset, and A. Levy Yeyati, Phys. Rev. Lett. **111**, 136806 (2013).
[10] F. Rossella, A. Bertoni, D. Ercolani, M. Rontani, L. Sorba, F. Beltram, and S. Roddaro, Nature Nano **9**, 997 (2014).
[11] R. S. Deacon, A. Oiwa, J. Sailer, S. Baba, Y. Kanai, K. Shibata, K. Hirakawa, and S. Tarucha, Nature Commun. **6**, 7446 (2015).
[12] P. Marra, R. Citro, and A. Braggio, Phys. Rev. B **93**, 220507 (2016).
[13] J. Tiira, E. Strambini, M. Amado, S. Roddaro, P. San-Jose, R. Aguado, F. S. Bergeret, D. Ercolani, L. Sorba, and F. Giazotto, Nature Commun. **8**, 14984 (2017).
[14] J. Linder and J. W. A. Robinson, Nature Phys. **11**, 307 (2015).
[15] C. Monroe, Nature **416**, 238 (2002).
[16] T. D. Ladd, F. Jelezko, R. Laflamme, Y. Nakamura, C. Monroe, and J. L. O'Brien, Nature **464**, 45 (2010).
[17] D. Beckmann, H. B. Weber, and H. v. Löhneysen, Phys. Rev. Lett. **93**, 197003 (2004).
[18] L. Hofstetter, A. Geresdi, M. Aagesen, J. Nygård, C. Schönenberger, and S. Csonka, Phys. Rev. Lett. **104**, 246804 (2010).
[19] P. Trocha and I. Weymann, Phys. Rev. B **91**, 235424 (2015).
[20] K. Wrześniewski, P. Trocha, and I. Weymann, J. Phys.: Condens. Matter **29**, 195302 (2017).
[21] K. Bocian, W. Rudziński, and I. Weymann, Phys. Rev. B **97**, 195441 (2018).
[22] M.-S. Choi, C. Bruder, and D. Loss, Phys. Rev. B **62**, 13569 (2000).
[23] P. Recher, E. V. Sukhorukov, and D. Loss, Phys. Rev. B **63**, 165314 (2001).
[24] O. Sauret, D. Feinberg, and T. Martin, Phys. Rev. B **70**, 245313 (2004).
[25] L. Hofstetter, S. Csonka, J. Nygard, and C. Schönenberger, Nature **461**, 960 (2009).
[26] L. G. Herrmann, F. Portier, P. Roche, A. L. Yeyati, T. Kontos, and C. Strunk, Phys. Rev. Lett. **104**, 026801 (2010).
[27] J. Schindele, A. Baumgartner, R. Maurand, M. Weiss, and C. Schönenberger, Phys. Rev. B **89**, 045422 (2014).
[28] G. Fülöp, F. Domínguez, S. d'Hollosy, A. Baumgartner, P. Makk, M. H. Madsen, V. A. Guzenko, J. Nygård, C. Schönenberger, A. Levy Yeyati, and S. Csonka, Phys. Rev. Lett. **115**, 227003 (2015).
[29] R. Hussein, L. Jaurigue, M. Governale, and A. Braggio, Phys. Rev. B **94**, 235134 (2016).
[30] R. Hussein, A. Braggio, and M. Governale, Phys. Status Solidi B **254**, 1600603 (2017).
[31] H. B. Radousky and H. Liang, Nanotechnology **23**, 502001 (2012).
[32] B. Roche, P. Roulleau, T. Jullien, Y. Jompol, I. Farrer, D. Ritchie, and D. Glattli, Nature Commun. **6**, 6738 (2015).
[33] H. Thierschmann, R. Sánchez, B. Sothmann, F. Arnold, C. Heyn, W. Hansen, H. Buhmann, and L. W. Molenkamp, Nature Nanotech. **10**, 854 (2015).
[34] J. Mastomäki, S. Roddaro, M. Rocci, V. Zannier, D. Ercolani, L. Sorba, I. J. Maasilta, N. Ligato, A. Fornieri, E. Strambini, and F. Giazotto, Nano Res. **10**, 3468 (2017).
[35] P. Virtanen and T. T. Heikkilä, Phys. Rev. Lett. **92**, 177004 (2004).
[36] P. Machon, M. Eschrig, and W. Belzig, Phys. Rev. Lett. **110**, 047002 (2013).
[37] P. Machon, M. Eschrig, and W. Belzig, New J. Phys. **16**, 073002 (2014).
[38] A. Ozaeta, P. Virtanen, F. S. Bergeret, and T. T. Heikkilä, Phys. Rev. Lett. **112**, 057001 (2014).
[39] F. Giazotto, P. Solinas, A. Braggio, and F. S. Bergeret, Phys. Rev. Applied **4**, 044016 (2015).
[40] F. Giazotto, T. T. Heikkilä, and F. S. Bergeret, Phys. Rev. Lett. **114**, 067001 (2015).
[41] J. Linder and M. E. Bathen, Phys. Rev. B **93**, 224509 (2016).
[42] S.-Y. Hwang, R. López, and D. Sánchez, Phys. Rev. B **91**, 104518 (2015).
[43] S.-Y. Hwang, R. López, and D. Sánchez, Phys. Rev. B **94**, 054506 (2016).
[44] C. Van den Broeck, Phys. Rev. Lett. **95**, 190602 (2005).
[45] B. Muralidharan and M. Grifoni, Phys. Rev. B **85**, 155423 (2012).
[46] F. Mazza, R. Bosisio, G. Benenti, V. Giovannetti, R. Fazio, and F. Taddei, New J. Phys. **16**, 085001 (2014).
[47] R. S. Whitney, Phys. Rev. Lett. **112**, 130601 (2014).
[48] G. Benenti, G. Casati, K. Saito, and R. S. Whitney, Phys. Rep. **694**, 1 (2017).
[49] L. Karwacki and P. Trocha, Phys. Rev. B **94**, 085418 (2016).
[50] P. A. Erdman, F. Mazza, R. Bosisio, G. Benenti, R. Fazio, and F. Taddei, Phys. Rev. B **95**, 245432 (2017).
[51] Z. Cao, T.-F. Fang, L. Li, and H.-G. Luo, Appl. Phys. Lett. **107**, 212601 (2015).
[52] A. V. Rozhkov and D. P. Arovas, Phys. Rev. B **62**, 6687 (2000).
[53] T. Meng, S. Florens, and P. Simon, Phys. Rev. B **79**, 224521 (2009).
[54] J. Eldridge, M. G. Pala, M. Governale, and J. König, Phys. Rev. B **82**, 184507 (2010).
[55] A. Braggio, M. Governale, M. G. Pala, and J. König, Solid State Commun. **151**, 155 (2011).
[56] B. Sothmann, S. Weiss, M. Governale, and J. König, Phys. Rev. B **90**, 220501 (2014).
[57] S. Weiss and J. König, Phys. Rev. B **96**, 064529 (2017).
[58] N. Walldorf, C. Padurariu, A.-P. Jauho, and C. Flindt, Phys. Rev. Lett. **120**, 087701 (2018).
[59] K. Saito and A. Dhar, Phys. Rev. Lett. **99**, 180601 (2007).
[60] K. Saito and Y. Utsumi, Phys. Rev. B **78**, 115429 (2008).
[61] R. Hussein and S. Kohler, Phys. Rev. B **89**, 205424 (2014).
[62] D. A. Bagrets and Yu. V. Nazarov, Phys. Rev. B **67**, 085316 (2003).
[63] A. Braggio, J. König, and R. Fazio, Phys. Rev. Lett. **96**, 026805 (2006).
[64] R. Sánchez and M. Büttiker, Europhys. Lett. **100**, 47008 (2012).
[65] S. Gasparinetti, P. Solinas, A. Braggio, and M. Sassetti, New J. Phys. **16**, 115001 (2014).
[66] In principle a full investigation at finite U_α can be performed, see Ref. 29.
[67] The simplicity of this picture is due to the absence of the double occupancy of the individual dots, which is energetically forbidden by the strong interaction.
[68] C. W. J. Beenakker, Phys. Rev. B **44**, 1646 (1991).
[69] M. Turek and K. A. Matveev, Phys. Rev. B **65**, 115332 (2002).

[70] N. Nakpathomkun, H. Q. Xu, and H. Linke, Phys. Rev. B **82**, 235428 (2010).
[71] Y. Dubi and M. Di Ventra, Rev. Mod. Phys. **83**, 131 (2011).
[72] C. Eltschka, H. Thierschmann, H. Buhmann, and J. Siewert, Phys. Status Solidi A **213**, 626 (2016).
[73] F. Mazza, S. Valentini, R. Bosisio, G. Benenti, V. Giovannetti, R. Fazio, and F. Taddei, Phys. Rev. B **91**, 245435 (2015).
[74] J. Splettstoesser, M. Governale, J. König, F. Taddei, and R. Fazio, Phys. Rev. B **75**, 235302 (2007).
[75] In order to have a finite nonlocal coupling Γ_S both the two local coupling $\Gamma_{S\alpha}$ with the superconductor need to be finite as $\Gamma_S \propto \Gamma_{SR}\Gamma_{SL}$.
[76] M. Rey and F. Sols, Phys. Rev. B **70**, 125315 (2004).
[77] R. Sánchez, P. Burset, and A. Levy Yeyati, arXiv:1806.04035 (2018).